Spacecraft observations of electromagnetic perturbations connected with seismic activity

František Němec, Ondrej Santolík, Michel Parrot, Jean-Jacques Berthelier

Spacecraft observations of electromagnetic perturbations connected with seismic activity

F. Němec,[1,2,3] O. Santolík,[3,4] M. Parrot,[1] and J. J. Berthelier[5]

Received 31 October 2007; revised 29 January 2008; accepted 12 February 2008; published 15 March 2008.

[1] Results of a statistical study of intensity of VLF electromagnetic waves observed in the vicinity of earthquakes are presented. A unique set of data obtained by the micro-satellite DEMETER (altitude of about 700 km, nearly Sun-synchronous orbit) and a robust two-step data processing has been used. In the first step, all the measured data are used to construct a map of electromagnetic emissions containing a statistical description of wave intensity at a given point of the satellite orbit under given conditions. In the second step, the intensity measured close to earthquakes is analyzed using the statistical distribution of background intensity obtained in the first step. The changes of wave intensity caused by seismic activity are investigated and their statistical significance is evaluated. Altogether, more than 2.5 years of satellite data have been analyzed and about 9000 earthquakes with magnitudes larger than or equal to 4.8 that occurred all over the world during the analyzed period have been included in the study. It is shown that, during the night, there is a statistically significant decrease by 4 – 6 dB of the measured wave intensity shortly (0–4 hours) before an intense surface (depth less than or equal to 40 km) earthquake. **Citation:** Němec, F., O. Santolík, M. Parrot, and J. J. Berthelier (2008), Spacecraft observations of electromagnetic perturbations connected with seismic activity, *Geophys. Res. Lett.*, *35*, L05109, doi:10.1029/2007GL032517.

1. Introduction

[2] Electromagnetic perturbations possibly connected with seismic activity have been in the recent years reported by several authors, both from ground based measurements [*Tate and Daily*, 1989; *Asada et al.*, 2001] and from low-altitude satellite experiments [*Parrot and Mogilevsky*, 1989; *Larkina et al.*, 1989; *Molchanov et al.*, 1993; *Parrot*, 1994; *Hobara et al.*, 2005; *Molchanov et al.*, 2006]. These observations have been the subject of an intense debate in the literature [see, e.g., *Rodger et al.*, 1996] for two main reasons. The first one stems from the lack of large and reliable database: most studies in this area have been limited by a lack of enough experimental results to conduct a statistically significant analysis of the phenomena and obtain firm results. In addition, the theoretical ideas [*Molchanov et al.*, 1995; *Sorokin et al.*, 2001] and physical mechanisms [*Gershenzon et al.*, 1989; *Molchanov and Hayakawa*, 1998] that have been proposed are not convincing enough since they lack the support of reliable experimental evidence.

[3] Using a survey of electromagnetic emissions on a low-altitude satellite that includes the vast majority of orbits that occurred over 2.5 years, we have been able to perform a unique statistical study of the influence of seismic activity on the intensity of electromagnetic waves in the ionosphere.

2. Data Set

[4] Our study is based on the data from the French micro-satellite DEMETER, launched in June, 2004 on a quasi helio-synchronous circular orbit (10.30–22.30 LT) with a 98° inclination and an altitude of about 700 km [*Parrot et al.*, 2006]. It performs 14 orbits per day and the instruments are nearly continuously powered at geomagnetic latitudes between −65° to +65° thus providing a very good coverage of the Earth's seismic zones. We have used the electric and magnetic field data from the ICE [*Berthelier et al.*, 2006] and IMSC [*Parrot et al.*, 2006; *Santolík et al.*, 2006] experiments, respectively, and, more specifically, the measurements made in the VLF band (from 15 Hz to 17.4 kHz). Irrespective of the mode of operation of the satellite, power spectra of one electric and one magnetic field component are computed on-board with a frequency resolution of 19.5 Hz and a time resolution of 2 s or 0.5 s depending on the mode of operation. For the data set used in this study the selected electric component is perpendicular to the orbit plane and the magnetic field component is inclined by 45 degrees from the velocity vector direction. Data from more than 2.5 years of the satellite observations have been used, altogether representing about 11500 hours of observations organized in about 20000 half-orbits. According to the USGS catalog (http://neic.usgs.gov/neis/epic/epic_global.html), about 9000 earthquakes with magnitude larger than or equal to 4.8 occurred all over the world during the analyzed period.

3. Method of Analysis

[5] In order to search for a trend in the behavior of electromagnetic emissions above seismic regions, it is necessary to define the statistical distribution of the wave intensity in absence of seismic activity. As the first step of the data processing, we thus built a map of electromagnetic emissions, which contains a statistical description of the intensity of electromagnetic waves obtained from the entire 11500-hour data set. It can be represented by a 6-dimensional matrix. Two dimensions are the geomagnetic longitude and

[1]LPCE, CNRS, Orléans, France.
[2]Faculty of Mathematics and Physics, Charles University, Prague, Czech Republic.
[3]IAP, ASCR, Prague, Czech Republic.
[4]Also at Faculty of Mathematics and Physics, Charles University, Prague, Czech Republic.
[5]CETP, CNRS, Saint-Maur des Fossés, France.

0094-8276/08/2007GL032517

latitude of the satellite with a resolution of 10 and 2 degrees, respectively. The third dimension is the frequency. We limit our analysis to frequency range below 10 kHz in order to avoid frequencies of terrestrial VLF transmitters. We have selected 16 and 13 frequency bands (117 Hz each) for the electric and magnetic field, respectively, in such a way that these omit spacecraft interferences and cover the entire studied frequency range as uniformly as possible. The lower number of chosen frequency bands for magnetic field data is caused by a significantly larger amount of interferences, which makes the suitable choice much more difficult. The last 3 dimensions describe the magnetospheric conditions at the time of observation: Kp index for the quiet (0–1o) moderate (1+–2+) and disturbed (above 3−) geomagnetic conditions; magnetic local time (dayside and nightside), and season of the year (October–April, May–September). In each cell of this matrix we accumulate a histogram of the common logarithm of the intensity at a given place and under given conditions, using all the available data. For a given spacecraft location and magnetospheric conditions this results into an estimate of the probability density function $f(E)$ of observing a power spectral density E.

[6] The basic idea of the second step of our procedure is as follows. For a measured power spectral density of electric (magnetic) field fluctuations E_i, we determine its cumulative probability F_i as the value of the corresponding cumulative distribution function. This can be calculated as an integral of the probability density function f_i obtained for the same frequency and spacecraft location under similar magnetospheric conditions:

$$F_i = \int_{-\infty}^{E_i} f(E)\, dE \qquad (1)$$

[7] In other words, this is the probability (a number between 0 and 1) of occurrence of signals with an intensity less or equal to the measured level.

[8] We calculate these cumulative probabilities for measurements of wave intensity recorded during seismic events. We select the data points for which the vertical projection of the spacecraft position to the ground was closer than 1100 km to the epicenter of an earthquake and which were measured no more than 5 days before and 3 days after the main shock. If two or more different earthquakes occur close enough, and therefore possibly influence the data, the measurement is not taken into account. This condition is equivalent to taking into account only "individually occurring" earthquakes, sufficiently separated one from another either in time or in space. Consequently, sequences of earthquakes occurring at about the same time and the same location (typically the main shock and aftershocks) are not considered and data measured in their vicinity are not used. This is done in order to not mix pre- and post- seismic effects.

[9] The obtained cumulative probabilities are organized in bins as a function of: frequency (16/13 selected bands), time to/from an earthquake (resolution of 4 hours) and distance from an earthquake (resolution of 110 km). For a bin b we define a "probabilistic intensity" as follows:

$$I_b = \frac{\sum_{i=1}^{M_b} F_i}{M_b} - 0.5 \qquad (2)$$

where M_b is the number of cumulative probabilities F_i collected in a given bin. Now, if the observed intensities were significantly lower or larger than the usual ones, the attributed cumulative probabilities would be significantly different from 0.5 and the resulting probabilistic intensity would be significantly different from 0. In this way, we neutralize the influence of the distribution of intensities of natural waves on the resulting statistics. However, one problem remains: what quantitative value should we attribute to the word "significantly"? The answer can be found using basic statistical properties of the probabilistic intensity.

[10] If we calculate values of the cumulative probability from the entire original data set (not just from the selected earthquake cases), we obtain a large set of values which are uniformly distributed between 0 and 1. This is a trivial consequence of the definition of the cumulative distribution function [*Press et al.*, 1992]. Averaging them into the finite bins in position and time we sum a large number of these values. Consequently, according to the central limit theorem and supposing that M_b is sufficiently large, values of I_b follow the normal distribution with a mean value 0 and a standard deviation σ_b. If all the values F_i were independent, an estimate of σ_b would read

$$\sigma'_b = \frac{1}{\sqrt{12 M_b}} \qquad (3)$$

[11] The problem when performing this calculation is that although we know the total number of cumulative probabilities in the bin M_b, we do not know how many of them can be considered as independent. We can define this number of independent cumulative probabilities as M'_b.

[12] An estimate of M'_b should be derived from the number of continuous data intervals contained in a given bin. These continuous data intervals correspond to different half-orbits of the spacecraft. Duration of a half-orbit is about 35 minutes, which is longer than a typical time scale of intensity changes of electromagnetic waves in the upper ionosphere. Moreover, data from two successive orbits cannot be contained in the same bin. The number N_b of half-orbits contributing to a given bin could be thus considered as a lower estimate of M'_b,

$$M'_b = \frac{N_b}{\alpha^2}, \qquad (4)$$

where $\alpha \leq 1$ is a positive number defining which relative fraction of the data from a single half-orbit can be on average considered as independent. In other words, α is the same for all the bins and represents a measure of stability of electromagnetic waves: the lower the α is, the more variable is their intensity.

[13] This provides us with an estimate of σ_b which is based on the known number N_b of half-orbits contributing to a given bin,

$$\hat{\sigma}_b = \frac{\alpha}{\sqrt{12\, N_b}}, \qquad (5)$$

where α can then be estimated experimentally. The simplest approach is to select a set of bins and to suppose that the

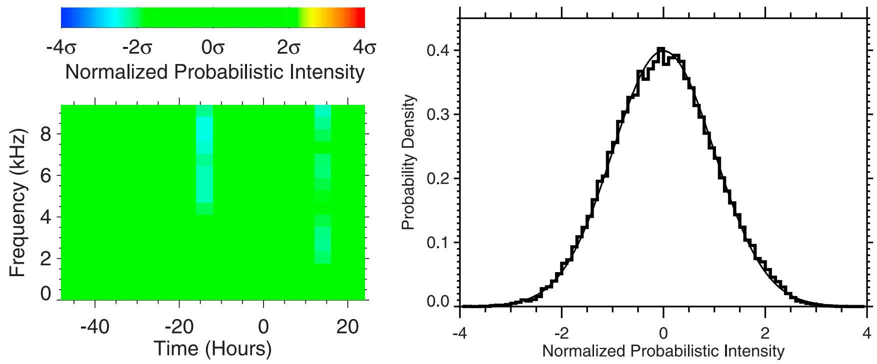

Figure 1. (left) Results from a superposed epoch method showing an example frequency-time spectrogram of normalized probabilistic intensity constructed from randomly distributed time intervals. The number and length of the time intervals corresponds to those used in the left panel of Figure 2. (right) Histogram of values of normalized probabilistic intensity obtained from randomly distributed time intervals of DEMETER data (obtained by combining 144 plots similar to the one shown in the left panel together). Over-plotted is a Gaussian distribution with mean value 0 and standard deviation 1 to demonstrate that the normalized probabilistic intensity follows this distribution.

standard deviation of the normalized probabilistic intensities I_b/σ_b should be unity within this set of bins. Since the mean value of I_b/σ_b should be zero, this leads us to an estimate of α,

$$\alpha = \sqrt{\frac{12}{Q}\sum_{b=1}^{Q} N_b I_b^2}, \qquad (6)$$

where Q is the number of bins in the set.

[14] In the paper, the values of the normalized probabilistic intensity are evaluated for Q = 48 time bins going from 5 days before an earthquake to 3 days after it, each bin representing 4 hours of time difference. This enables us to define α (the same for all the 48 time bins), calculate $\hat{\sigma}_b$ from equation (5), and to obtain the normalized probabilistic intensities I_b/σ_b for all the bins. These are then displayed in Figures 1, 2, and 3. If systematic deviations of several standard deviations ($>3\sigma_b$) are observed, we can consider the effect to be statistically significant.

[15] The correctness of the statistical analysis is demonstrated in Figure 1, which represents the results obtained from randomly distributed time intervals of the DEMETER data. Left panel shows an example frequency-time spectrogram of normalized probabilistic intensity in order to demonstrate that the expected random fluctuations of normalized probabilistic intensity (in the absence of seismic effects) do not display any particular variation. A histogram of values of normalized probabilistic intensity is plotted in the right-hand panel. It was obtained by combining 144 plots similar to the one shown in the left-hand panel and shows a Gaussian distribution with a mean value 0 and a standard deviation 1. Additional tests have been performed by applying the data processing method to random earthquake databases constructed by: 1) keeping real locations of earthquakes, but randomly generating their times 2) keeping real times of earthquakes, but randomly

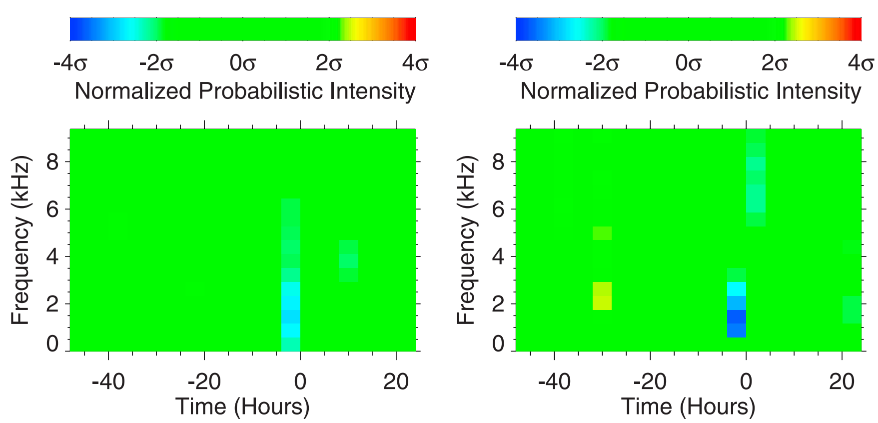

Figure 2. (left) Frequency-time spectrogram of the normalized probabilistic intensity (see text) obtained from the night-time electric field data measured within 330 km of the earthquakes with magnitudes larger than or equal to 4.8 and depth less than or equal to 40 km. Data measured for all Kp values and seasons have been included. (right) The same but for earthquakes with magnitudes larger than or equal to 5.0.

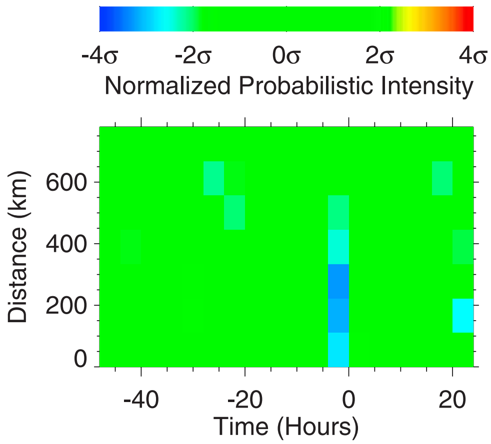

Figure 3. Normalized probabilistic intensity (see text) obtained from the night-time electric field data measured for earthquakes with magnitude larger than or equal to 5.0 and depth less than or equal to 40 km plotted as a function of the distance from the epicenters and of time from the earthquakes for a frequency band 1055–2383 Hz. Data measured for all Kp values and seasons have been included.

generating their positions. Again, no particular variation has been observed.

4. Results

[16] Since it has been reported that a depth of earthquakes can play a significant role in earthquake-related effects [e.g., *Rodger et al. 1999*], we have divided the earthquakes into two groups: surface earthquakes (depth less than or equal to 40 km) and deep earthquakes (depth larger than 40 km). Moreover, day-time and night-time data have been treated separately. Finally, all 4 different combinations of surface/deep earthquakes and day-time/night-time data have been examined for the presence of possible seismic effects.

[17] Figure 2 shows that the normalized probabilistic intensity obtained from the night-time electric field data is below the "normal" level shortly (0–4 hours) before the surface earthquakes at frequencies of about 1–2 kHz. The probabilistic intensity decreases by about 3 standard deviations for earthquakes with magnitudes larger than or equal to 4.8. This effect is based on the data collected during 50 different orbits. If we consider only surface earthquakes with magnitudes larger than or equal to 5.0, the effect becomes stronger, with the probabilistic intensity decreasing by about 4 standard deviations, and with 34 different orbits contributing to the bins where the decrease is detected. Concerning the probabilistic intensities, these correspond to values between −0.10 and −0.15. Transforming these values back to the corresponding power spectral density, we obtain a decrease between −4 and −6 dB. The decrease was observed also in the magnetic field data, but it is much weaker and its statistical significance is questionable. This can be probably explained by a lower sensitivity of magnetic field instrument and is not connected with the nature of intensity decrease. No similar effects were observed during the day (not shown). No effects were observed for deep earthquakes (not shown).

[18] Figure 3 shows that the spatial scale of the affected area is approximately 350 km (however, one should keep in mind that the spatial resolution of our bins is only about 110 km, which place rather large uncertainties on the result). This corresponds relatively well to the size of the earthquake preparation zone estimated using the *Dobrovolsky et al.* [1979] formula: 140 km for earthquakes with magnitudes 5.0 and 380 km for earthquakes with magnitudes 6.0.

5. Discussion and Summary

[19] The presented statistical study disagrees with previous systematic studies that claimed the presence of seismic effects since they mostly reported an increase in the ELF/VLF activity [*Larkina et al.*, 1989; *Parrot and Mogilevsky*, 1989; *Serebryakova et al.*, 1992; *Molchanov et al.*, 1993; *Parrot*, 1994]. These studies have been critically examined by *Henderson et al.* [1993], who underlined the importance of usage of control set of data in order to estimate statistical significance of the observed effects and who failed to indicate any significant differences between the earthquake and control orbits. More recently, a similar result was obtained by *Rodger et al.* [1996]. However, as noted by *Parrot* [1999], both these studies probably could not detect decreases in wave activity and can be therefore considered as being in agreement with our study.

[20] There are two basic possibilities for the explanation of the observed decrease: naturally occurring waves are either attenuated or diverged over earthquake epicenters (this could be caused by a decrease of the refractive index, as proposed by *Vodyanitskii et al.* [1990]). A possible explanation of why the decrease is observed only in the night-time data could be that during the day the ionospheric ionization is significantly larger. Any potential changes caused by seismic activity may be thus overwhelmed by this stronger influence. It is also important to note that the frequency band where the decrease is observed could be related to the cut-off frequency of the first TM mode in the Earth-ionosphere guide (1.7 kHz during the night-time). Finally, our analysis shows that the effect is connected only with surface earthquakes, as suggested by previous researchers [see, e.g., *Rodger et al.*, 1999, and references therein].

[21] We have statistically demonstrated that a significant intensity decrease is observed in night-time data shortly before the main shock of large surface earthquakes. Further research based on the increasing data set of DEMETER measurements will hopefully help us to understand its nature.

[22] **Acknowledgments.** FN and OS acknowledge support of the GACR grant 205/06/1267.

References

Asada, T., H. Baba, M. Kawazoe, and M. Sugiura (2001), An attempt to delineate very low frequency electromagnetic signals associated with earthquakes, *Earth Planets Space*, *53*, 55–62.

Berthelier, J. J., et al. (2006), ICE, the electric field experiment on DEMETER, *Planet. Space Sci.*, *54*, 456–471.

Dobrovolsky, I. R., S. I. Zubkov, and V. I. Myachkin (1979), Estimation of the size of earthquake preparation zones, *Pure Appl. Geophys.*, *117*, 1025–1044.

Gershenzon, N. I., M. B. Gokhberg, A. V. Karakin, N. V. Petviashvili, and A. L. Rykunov (1989), Modelling the connection between earthquake preparation processes and crustal electromagnetic emission, *Phys. Earth Planet. Inter.*, *57*, 129–138.

Henderson, T. R., V. S. Sonwalkar, R. A. Helliwell, U. S. Inan, and A. C. Fraser-Smith (1993), A search for ELF/VLF emissions induced by earthquakes as observed in the ionosphere by the DE 2 satellite, *J. Geophys. Res.*, *98*(A6), 9503–9514.

Hobara, Y., F. Lefeuvre, M. Parrot, and O. A. Molchanov (2005), Low-latitude ionospheric turbulence observed by Aureol-3 satellite, *Ann. Geophys.*, *23*, 1259–1270.

Larkina, V. I., V. V. Migulin, O. A. Molchanov, I. P. Kharkov, A. S. Inchin, and V. B. Schvetcova (1989), Some statistical results on very low frequency radiowave emissions in the upper ionosphere over earthquake zones, *Phys. Earth Planet. Inter.*, *57*, 100–109.

Molchanov, O. A., and M. Hayakawa (1998), On the generation mechanism of ULF seismogenic electromagnetic emissions, *Phys. Earth Planet. Inter.*, *105*, 201–210.

Molchanov, O. A., O. A. Mazhaeva, A. N. Goliavin, and M. Hayakawa (1993), Observation by the Intercosmos-24 satellite of ELF-VLF electromagnetic emissions associated with earthquakes, *Ann. Geophys.*, *11*, 431–440.

Molchanov, O. A., M. Hayakawa, and V. A. Rafalsky (1995), Penetration characteristics of electromagnetic emissions from an underground seismic source into the atmosphere, ionosphere, and magnetosphere, *J. Geophys. Res.*, *100*(A2), 1691–1712.

Molchanov, O., et al. (2006), Global diagnostics of the ionospheric perturbations related to the seismic activity using the VLF radio signals collected on the DEMETER satellite, *Nat. Hazards Earth Syst. Sci.*, *6*, 745–753.

Parrot, M. (1994), Statistical study of ELF/VLF emissions recorded by a low-altitude satellite during seismic events, *J. Geophys. Res.*, *99*, 23,339–23,347.

Parrot, M. (1999), Statistical studies with satellite observations of seismogenic effects, in *Atmospheric and Ionospheric Electromagnetic Phenomena Associated with Earthquakes*, edited by M. Hayakawa, pp. 685–695, Terra Sci., Tokyo.

Parrot, M., and M. M. Mogilevsky (1989), VLF emissions associated with earthquakes and observed in the ionosphere and the magnetosphere, *Phys. Earth Planet. Inter.*, *57*, 86–99.

Parrot, M., et al. (2006), The magnetic field experiment IMSC and its data processing onboard DEMETER: Scientific objectives, description and first results, *Planet. Space Sci.*, *54*, 441–455.

Press, W. H., S. A. Teukolsky, W. T. Vetterling, and B. P. Flannery (1992), Random numbers, in *Numerical Recipes in C: The Art of Scientific Computing*, pp. 274–328, Cambridge Univ. Press, New York.

Rodger, C. J., N. R. Thomson, and R. L. Dowden (1996), A search for ELF/VLF activity associated with earthquakes using ISIS satellite data, *J. Geophys. Res.*, *101*(A6), 13,369–13,378.

Rodger, C. J., R. L. Dowden, and N. R. Thomson (1999), Observations of electromagnetic activity associated with earthquakes by low-altitude satellites, in *Atmospheric and Ionospheric Electromagnetic Phenomena Associated with Earthquakes*, edited by M. Hayakawa, pp. 697–710, Terra Sci., Tokyo.

Santolík, O., F. Němec, M. Parrot, D. Lagoutte, L. Madrias, and J. J. Berthelier (2006), Analysis methods for multi-component wave measurements on board the DEMETER spacecraft, *Planet. Space Sci.*, *54*, 512–527.

Serebryakova, O. N., S. V. Bilichenko, V. M. Chmyrev, M. Parrot, L. Rauch, F. Lefeuvre, and O. A. Pokhotelov (1992), Electrodynamic ELF radiation from earthquake regions as observed by low-altitude satellites, *Geophys. Res. Lett.*, *19*, 91–94.

Sorokin, V. M., V. M. Chmyrev, and A. K. Yaschenko (2001), Electrodynamic model of the lower atmosphere and the ionosphere coupling, *J. Atmos. Sol. Terr. Phys.*, *63*, 1681–1691.

Tate, J., and W. Daily (1989), Evidence of electro-seismic phenomena, *Phys. Earth Planet. Inter.*, *57*, 1–10.

Vodyanitskii, S. Y., A. I. Daniluskin, V. V. Krasnoselskikh, V. V. Migulin, P. A. Morozov, A. M. Natanzon, and A. E. Reznikov (1990), The change of the ELF-VLF noise level at the Earth's surface in a magnetic conjugate region during the Spacelab-2 experiment, *Adv. Space Res.*, *10*(7), 789–794.

J. J. Berthelier, CETP, CNRS, Saint-Maur des Fossés F-94100, France.

F. Němec and M. Parrot, LPCE, CNRS, Orléans F-45071, France. (frantisek.nemec@cnrs-orleans.fr)

O. Santolík, Institute of Atmospheric Physics, Academy of Sciences of the Czech Republic, Prague 4, 14131, Czech Republic.